IEEE/ IEEE/CSC & ESAS EUROPEAN SUPERCONDUCTIVITY NEWS FORUM, No. 12, April 2010
The published version of this manuscript appeared in IEEE Transactions on Applied Superconductivity **20**, No. 874 - 879 (2010)

HTS Magnetic Bearings in Prototype Application

Frank N. Werfel, Uta Floegel - Delor, Thomas Riedel, Rolf Rothfeld, Dieter Wippich, Bernd Goebel,

Abstract **- ATZ Company has successfully developed high temperature superconducting (HTS) magnetic bearings for power energy application and high-speed machinery. Journal–type design and improved HTS magnetic properties increasingly fulfil industrial prototype requirements. Maximum load up to 1.1 ton, stiffnesses in 3 – 4 kN/mm level, simultaneous self – stabilization in axial and radial directions, large- gap operation of 5- 6 mm and reliable machine cooling in the 50 – 60 K region characterize the present progress of HTS magnetic bearings. A 200 mm HTS bearing of 10 kN load capacity is fabricated and integrated in a 5 kWh/250 kW flywheel energy storage system. We report about a new large-gap HTS magnetic coupling system ensuring 300 mm wafer treatment inside a closed processing chamber in semiconductor industry. A linear MAGLEV transport system consisting of four modular cryostat units have been recently fabricated in a prototyping process. The four HTS cryostats can carry almost 1 ton at 10 mm magnetic gap above a magnetic guideway with a force density of about 5 N/cm². Due to perfect thermal insulation each cryostat operates more than 24 hours without refilling LN_2.**

Index Terms – **HTS magnetic bearing, flywheel, MAGLEV**

I. INTRODUCTION

Adelwitz Technologiezentrum (ATZ) is producing about 500 kg High Temperature Superconducting (HTS) powder of the REBCO type per annum for melt textured bulk and thin film / coated conductor application. About 60 % of the materials as melt textured single or multi-seed YBCO blocks are applied in HTS magnetic components and devices. Basic HTS elements of magnetic bearings consist of top –seeded melt textured YBCO bulks with two or three SmBCO seeds.

Due to the improved fabrication of bulk high temperature superconducting (HTS) material, the use of superconducting passive magnetic bearings (SMB`s) for rotational applications is increasingly becoming attractive. The basic physics of HTS magnet interaction has been investigated rather early after the HTS discovery [1-3]. Melt textured YBCO can be fabricated in single-grain structure and assembled in tiles shaped, in either planar- or cylinder–like devices.

Active magnetic bearings (AMB's) determine the technological level of magnetic bearing technique since about two decades. Substantial improvements of AMB's were achieved by progress in electronics and especially in mechatronics. A state- of- the –art AMB has a 0.6 mm free

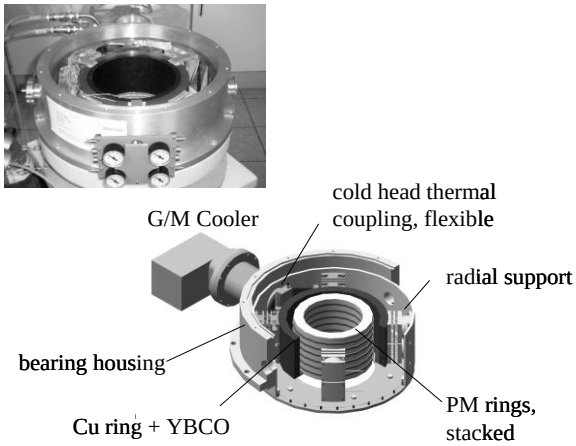

Fig. 1. Superconducting magnetic 1-ton bearing of HTS flywheel.

TABLE I. 1-TON HTS MAGNETIC BEARING

Design /Geometry, Diameter x height [mm]	Radial –type, 205 x 120
Magnetic area [cm²]	768
Superconductor	Melt textured YBCO, 3 seeds
HTS size / number of elements	65 x 35 x 13 / 55 pcs. glued in Cu - ring
Rotor configuration	200 mm x150 PM/ Fe collect.
Housing insulation	GfK /CfK
Magnetic gap	2.5 mm
Free rotor movement [mm]	2 mm radial
Force excitation	Rotor displacement (ax +rad)
Cooling	LN2 / sub LN2 (78 K +72 K)
Total bearing weight [kg]	55
Measured performance	
Maximum load, radially [N]	4700 at 3.2 mm displacement 72 K!
Maximum load , axially [N]	4600 / 1 mm, 10080 /3.3 mm
Stiffness, radially [kN/mm]	1.8 (72 K), 1.4 (79 K)
Rad stiffness symmetry	Radially homogenously
Stiffness axially [kN/mm]	4.5 (72 K), 3 (78.5 K)
Thermal losses [W]	< 20 W
Rotational friction [Nm]	- 5 x 10^{-4}

Manuscript received 20 October 2009. Flywheel development was supported by the German VDI / BMBF under the contract number 13N 8737 and 13N8738.

F. N. Werfel , U. Floegel - Delor, T. Riedel, R. Rothfeld, D. Wippich, and B. Goebel are with the Adelwitz Technologiezentrum GmbH (ATZ), Adelwitz, Germany, Phone +49 34222 45200, e-mail: werfel@t-online.de;

gap between rotor and stator and a force density up to 50 N/cm².

The principal benefit of SMB`s is comparable to those of AMB. The HTS magnetic bearings have to be cooled but are stable without electronics control. Their main advantages stem from low-drag torque and the self-centering, unlubricated, wear–free and vacuum-compatible operation. Particularly, radial-type HTS bearings are compact and robust in design, suitable for supporting high loads. However, in contrast to AMB bearings, superconducting magnetic bearings are self-regulated (by electromagnetic laws) without monitoring and electromagnetic regulation/ attraction of the rotor. Control and specification of the SMB properties such as levitation pressure (load), restoring forces (stiffness) and damping are determined by the magnetic interaction design. At present SMB compared to AMB have a factor 3-4 smaller force densities and stiffnesses due to the limited magnetization of the available PM rings.

We have constructed about 60 systems of HTS – PM bearings aimed for application in the fields of energy technique and mechanical engineering systems. Larger prototype bearings were built for a 5 kWh /250 kW HTS flywheel, a 400 kW motor, centrifuge application and for scientific instruments. The radial bearing design and the parameters to stabilize a 0.6 ton flywheel rotor are shown in Fig. 1 and in Table I.

In this paper we discuss and review the present status of self-stabilized superconducting passive magnetic bearings suspending technical wheels and rotors. With larger magnetic flux densities, e.g. provided by stronger PM and bulk superconductors HTS bearings will have substantially increased magnetic force parameters.

II. HTS MAGNETIC BEARING APPLICATION

A. Magnetic bearing concept

The principal force exerted by a magnet on a Superconductor is given by the gradient of the volume integral $F = -$

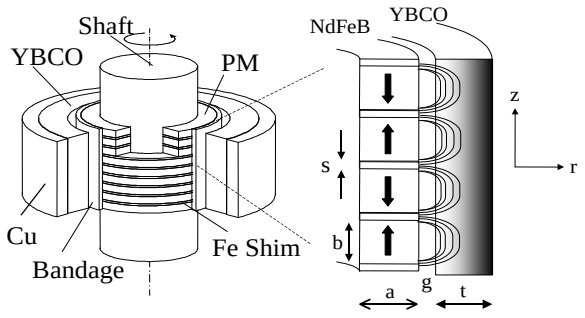

Fig. 2. HTS magnetic bearing design and interaction.

$grad \int (\boldsymbol{M} * \boldsymbol{B})\, dV$, where $\boldsymbol{M}$ is magnetic moment of the superconductor and $\boldsymbol{B}$ is the magnetic flux density produced by the PM configuration. The maximum levitation pressure is $P_{max} = B_r^2 / 2\,\mu_0$, if the critical current density is infinity ($\mu \rightarrow 0$). For the presently available high- energy PM`s (NdFeB, SmCo) with a surface induction B_r = 1.0 T, the magnetic pressure can reach a value of about 4 bar. The magnetic excitation of the bearing system can be determined by considering:

The field B(r, z) interacts with the YBCO superconductor. The exponential function exp(-πr/b) in the

Rotor: *Stack of alternating polarized permanent magnets PM with iron shims between. The magnetic components are given:*

Fourier field expansion:

$$\begin{Bmatrix} B_r \\ B_z \end{Bmatrix} = B(0)\exp(-\frac{\pi r}{b})\begin{Bmatrix} \sin \pi z/b \\ \cos \pi z/b \end{Bmatrix} + ...$$

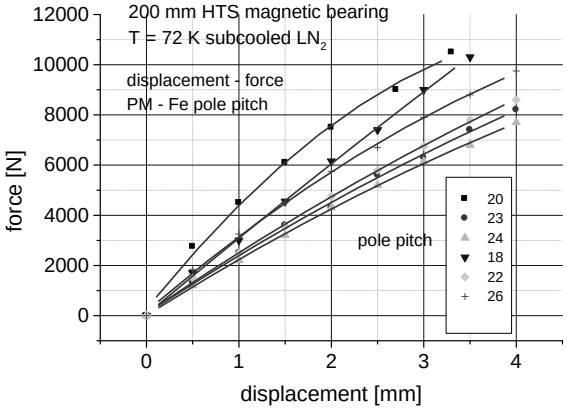

Fig. 3. Experimental displacement – force curves of the 200 mm flywheel HTS bearing at sub-cooled LN_2 (T=72 K) for different PM – Fe pole distances (pole pitch).

Fourier expansion describes the field gradient and determines the radial bearing stiffness $dF_{r/}$ dr which is proportional to the inverse PM stacking distance 1/b (b+s = pole pitch). Hereby are b and s in Fig. 2 the respective thicknesses of the PM rings and Fe collectors. The periodic sin/cos [πz/b] function characterizes the field variation in axial direction. This field variation generates persistence currents and gives the axial stiffness $dF_z/dz \propto 1/b$. An excellent overview about superconducting bearings is given in the Ref. [4] and [5].

The magnetic bearing concept depends strongly on the PM-Fe magnetic configuration as it is demonstrated by the force measurement in Fig. 3. For each magnetic gap exists exactly *one* optimum PM–Fe configuration, giving the highest magnetic force at displacement. In Fig. 3 a maximum axial force of more than 10 000 N at 3.3 mm displacement is obtained with an axial pole pitch distance b + s = 18-20 mm (Fig. 2).

B. Flywheel with HTS magnetic bearing

Flywheel developments with HTS bearings were started successfully in several groups [6, 7]. The here assembled HTS flywheel [8] without power electronics is presented in

Fig. 4. The flywheel cylindrical housing is fixed in a steel frame with four flexible carrying elements at the corners. Inside the container the components with the carbon / glass fiber rotor, the concentrically motor/generator and the two magnetic bearings are assembled on a central shaft. Two

Flywheel system:
-steel frame
-safety housing
-0.6 t rotor
-250 kW motor
-HTS bearing
-G/M cryo-cooler
-power electric
-safety equipment
-periphery
(vacuum, cooling)

Fig. 4. ATZ /MM flywheel with HTS magnetic bearing.

sets of dynamical emergency bearings and the magnetic bearings on the both ends of the shaft have to guarantee the precise mechanical adjustment during all rotor revolution speeds. The flywheel housing is evacuated by a rough / turbo-molecular pump combination to a basic vacuum of 10^{-2} -10^{-3} mbar. Friction experiments like in Chapter III, show the influence of air friction on the fast rotating surface of the rotor up to pressure of about 5 x 10^{-3} mbar. We developed and tested the radial HTS bearing with axial forces of 10 kN and 2-4 kN/mm axial stiffness (Fig. 5). Under vacuum it has an extremely low magnetic friction under rotation.

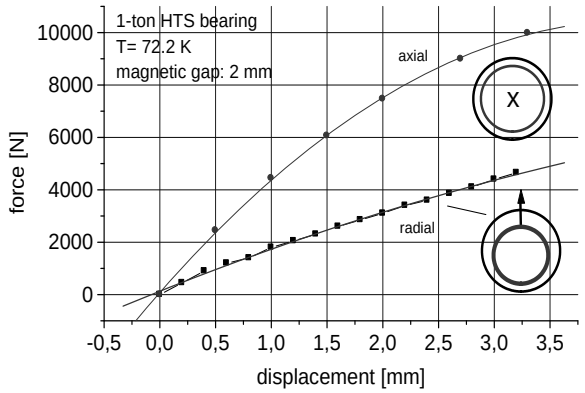

Fig. 5. Displacement –force measurements of the selected 1-ton HTS bearing in axial and radial direction.

Our technical concept with the HTS bearing on top and the PM bearing below the motor/generator was redesigned relative to the expected magnitude of the rotor vibration. Two dynamical dampers limit the rotor amplitudes passing the critical rpm (about 8 Hz). A corresponding effort in designing and testing HTS bearings is performed. At the rotor load of 0.6 ton the HTS bearing shows a displacement of about 1.5 mm. Together with negative stiffness of the PM bearing, located at the bottom of the flywheel, the rotor net displacement is less than 1 mm.

At 72 K the force - displacement curves in axial and radial direction of the 200 mm HTS magnetic bearing are shown in Fig. 5. With 3 mm vertical rotor displacement the HTS bearing can stabilize a maximum load of about 1 ton.

C. PM – HTS coupling

Magnetic couplers are well known in modern machinery to transfer forces or momentum forces from one element to another one without mechanical connection. However, these types of coupling are unstable in at least one geometrical direction. Either the magnets attract each other or show repulsive forces. Therefore, magnetic systems made of permanent magnets, need an additional stabilization either in radial or in axial direction. In contrast, the interaction between a superconductor and magnetic field result in a self –stabilization without additional effort.

Fig. 6 and Fig. 7 show a magnetic levitated systems operating through the bottom of a semiconductor processing chamber. The silicon wafer is fixed on a magnetic wafer carrier and rotated without any mechanical

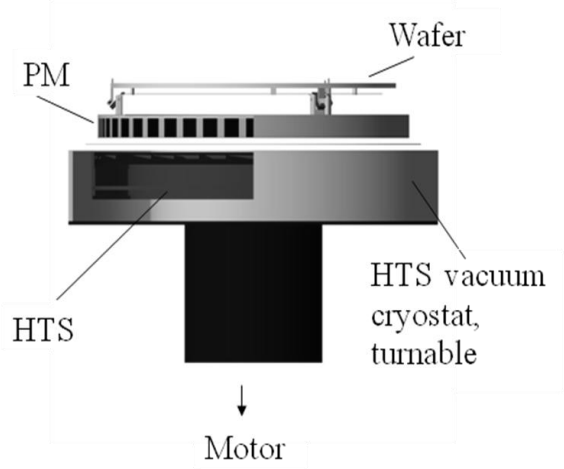

Fig. 6. PM – HTS magnetic coupler for semiconductor wafer treatment.

contact in a sealed chamber. The processing chamber, not shown in Fig. 6, is preferred in a shape of a Kloepper bottom to withstand mechanical vacuum or pressure forces at lowest wall thickness.

If a magnetic field in a superconductor is changed, i.e. due to strong displacement of a permanent magnet, in the superconducting material an electric field E>0 with an induced current density J > Jc is generated. Hereby is Jc the so-called critical current density of the superconducting material and determines the material quality.

For a coupling system the experimental magnet design has to be chosen a configuration with zero degree of freedom. The PM-HTS coupling strength in a first approach depends on the magnetic flux density in the gap and the

field dependent critical current density Jc of the superconductor.

As an example, in case of radial symmetric geometry one has to consider $dB/dr = \mu_0 Jc$, integrated in the Bean model gives $B^* = \mu_0$ Jc r for the maximum trapped magnetic flux B^*. Assuming a critical current Jc = 10^4 A/cm² and a grain diameter r = 20 mm, it gives a trapped field value $B^* = 1.2$ Tesla.

Utilizing this trapped flux, a HTS device as a stator and a magnetic rotor may be coupled in a non-contact one-by-one system At present the magnetic coupler distance is 13 mm. 12 PM's of the size 25.4 mm x 25.4 mm x 25.4 mm with an averaged surface magnetization of 540 mT are circularly arranged. At 13 mm distance the entrance flux density into the superconductor is about 170 mT, which is trapped into the YBCO stator. The neighbouring distance of the PM's on the circular holder should be larger than the magnet widths. The PM ring diameter with the carrier is d = 300 mm giving a high coupling torque M = F x d/2 (F magnetic force). Levitation force and torque allow a rotational speed of more than 1500 rpm of the wafer carrier in a chamber.

For safe operation, stator and rotor have to turn around a common center line without any mechanical contact. The coupling device may bridge a chamber wall. The air gaps between the rotating parts and the static chamber bottom

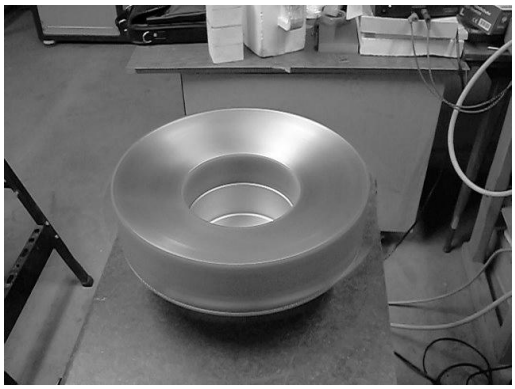

Fig. 7. Rotational HTS vacuum cryostat of magnetic coupler; diameter: 350 mm; LN_2 cooling.

should be small, e.g. 1-2 mm. Each movement of the stator is followed by an equivalent reaction of the rotor.

This HTS coupler combination provides suspension and propulsion simultaneously over distances of 5 – 30 mm. Its performance allows wet and gaseous chemical treatment under rotation in closed chambers without any shaft or intrinsic drive unit.

D. Linear MAGLEV

Superconducting Maglev trains in demonstrator version uses axial levitation forces [9]. The force is generated by a field cooled (fc) process at a distance of about 20 – 30 mm, whereby with load the gap decreases to 10 – 5 mm above the PM guideway. Although the total loads of different systems approach in between several hundred kilograms load (ASCLab Chengdu, China, U Rio de Janeiro, Brazil,

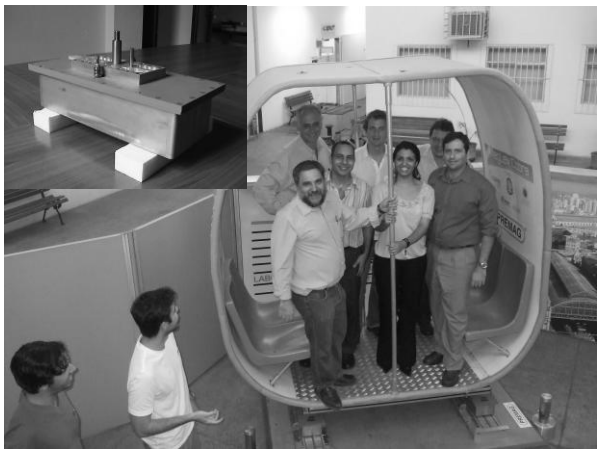

Fig. 8. Full-Scale Module of the Maglev-Cobra HTS-Superconducting Vehicle, U. Rio de Janeiro; Insert: MAGLEV HTS cryostat (ATZ).

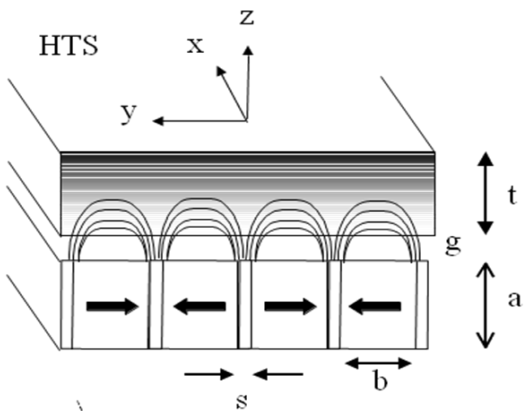

1. Field distribution above the guideway
Fourier development, first term is important

$$B_z = B_0 \exp(-\pi z / L) \sin(\pi y / L)$$

Flux density in normal direction

$$B_y = B_0 \exp(-\pi z / L) \cos(\pi y / L)$$

Flux density in tangential direction

2. (i) Magnetic flux density decays exponentially to the surface plane

(ii) The decay is at a distance comparable to the period of the magnetic poles L

3. $|B| = [B_z^2 + B_y^2]^{1/2}$

Absolute values of flux density

Fig. 9. General MAGLEV HTS - PM design; basic expressions about magnetic flux distribution

IFW Dresden, Germany, and Moscow, Russia), the force density values with 2 - 3 N/cm² are limited. In addition, large field cooled distances > 30 mm between magnetic guideway and superconductor show low stiffnesses and hence low guidance forces of the trains and vehicles. Fig. 8

shows a vehicle test module called COBRA type of the

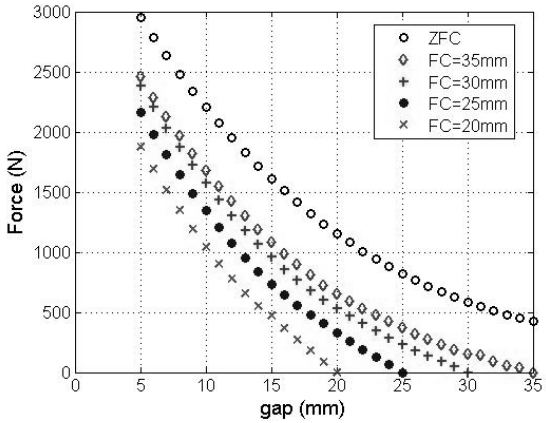

Fig. 10. Levitation force of MAGLEV cryostat at different field - cooled (fc) positions, and zero-field cooled (zfc).

University of Rio de Janeiro [10]. The vehicle is magnetically suspended by four HTS cryostats above a magnetic track. Each cryostat can have a load up to 0.25 t at 10 mm distance and operates with 2.5 l LN_2 more than one day. Two key components of the MAGLEV levitation

TABLE II: VACUUM CRYOSTAT/ST.STEEL Cu /YBCO

HTS	2 x 12 YBCO blocks
HTS area	492 cm²
Cooling	2.5 l LN_2,
Operat. time	> 24 h
Cryostat weight	~ 16 kg
Magn. Distance	2 mm distance bottom – YBCO
Levitation	~ 2500 N @10 mm; fc35
Force density	5N / cm²

system have to be solved: (i) Optimum magnetic configuration of the guideway, presently made by assembling of PM's and Fe collectors. (ii) Preparation of superconducting bulks with high current density and mechanical stability, assembled in a robust, moveable thermal insulating /vacuum housing.

The magnetic rail solutions are usually obtained by Electro-magnetic Finite Element Method (FEM) simulations. From this one can estimate in a first approach the field distribution above the track (Fig. 9). The FEM results show the magnetic flux lines and the magnetic flux density distribution. Soft magnetic bars, made of low-carbon steel, collect the flux and improve the magnetic gradients similar to the HTS rotational bearing situation in Fig. 2. The HTS–PM configuration is shown in Fig. 9, whereby the experimental force measurements of a cryostat with the parameters of Table II are given in Fig. 10.

Numerous configurations of PM's with Fe flux collectors or HALBACH configurations have been proposed. Practically, the levitation force at a certain distance determines the load performance of a MAGLEV train. The four YBCO cryostats assembled under the MAGLEV COBRA vehicle in Fig. 8 has been tested at different field cooling positions. The results are given in Fig. 10 and confirm the estimated maximum load of about 1 ton at 5-8 mm distance by the levitation of 4 HTS cryostats.

The technical parameters of the vacuum cryostats with the included melt textured YBCO blocks are summarized in Table II. An important feature is the small magnetic distance of about 2 mm between the (cold) surface of the YBCO blocks and the outer stainless steel bottom surface.

E. Magnetic platform

A simple HTS - magnet axial configuration has been constructed and assembled for a demonstration of magnetic levitation forces in Fig. 11. The platform is capable to levitate and rotate a person freely (man - loading platform). The platform consists of circular assembled melt textured YBCO blocks glued into a copper holder. The cryostat has a LN_2 storage container inside a vacuum compatible stainless steel (SS) and glass fiber housing. The PM's are mounted into ring holder fitting the HTS diameter. The HTS cryostat possesses a vacuum valve for maintenance of the thermal insulation vacuum. Two SS tubes go outside radially to the center for filling the LN_2 into the storage container. The cool –down procedure takes about 90 minutes, while the operation time can be 5-8 hours. The PM ring is typically fixed mechanically at 30-40 mm above the cryostat before cooling, and then after field-cooling procedure released. The platform with the present magnetic configuration was tested up to loads of about 100 kg.

Fig. 11. HTS magnetic platform demonstrating levitation forces.

III. DYNAMICAL BEARING EFFECTS

HTS magnetic bearings possess extremely low friction properties because of the non-contact behavior. Even at higher speeds the interacting surfaces don't need any lubrication and generate no friction heat. The rotor breaking effects are caused by air friction and by weak magnetic friction. The latter is mainly caused by hysteretic and eddy current effects due to magnetic inhomogeneities of the PM configuration.

Fig. 12 exhibits measured spin – down curves of the 200 mm flywheel bearing. It shows, that after acceleration to a certain speed, in the present case 2000 rpm, the 16 kg bearing rotor needs more than two hours to decelerate to zero rpm under vacuum condition of about 10^{-3} mbar. The HTS temperature was about 80 K. The linear behaviour of the rotor deceleration is mainly caused by a constant friction moment. By improving the magnetic homogeneity of the rotor ring magnets (Fig. 2), the losses can be further reduced. The breaking friction moment here is estimated from the curves in Fig. 12 to 5 x 10^{-4} Nm.

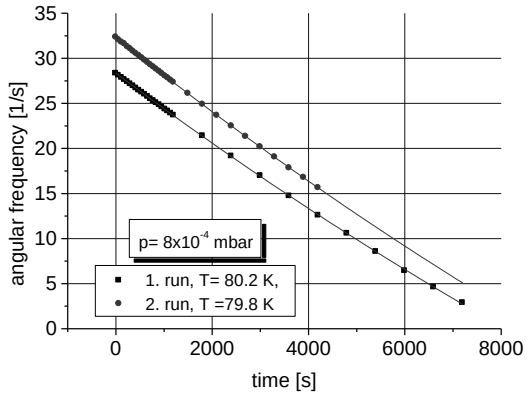

Fig. 12. Spin-down curve of the 200 mm bearing rotor.

IV. Magnetic Bearings With Incrased Force Density

The force and stiffness of a magnetic bearing depend on the magnetic flux density which is available for the magnetic interaction between rotor and stator. Permanent magnets are easy to handle, can be assembled in different configurations, and provide the magnetic flux density by their magnetization without additional electric biasing. The maximum force density of HTS – PM bearings is practically limited to about 5- 10 N/cm², which corresponds to a magnetic flux density excitation of about 0.5 T.

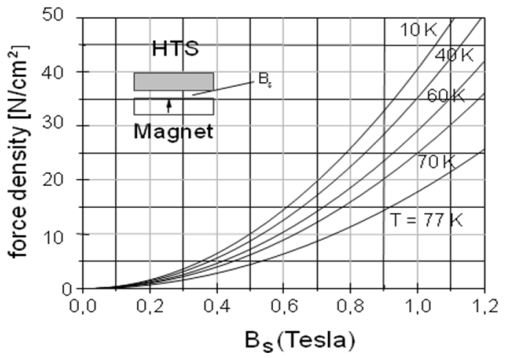

Fig. 13. Calculated magnetic force density with increased magnetic flux density between magnet and superconductor.

On the other hand, Active Magnetic Bearings (AMB) are specified with force densities up to 50 N/cm². With better PM material, shorter interaction distances and improved magnetic PM - Fe configurations, a higher magnetic flux density can be generated. A corresponding calculation of the magnetic force density at increased B values with lower HTS temperatures is given in Fig. 13.

V. Conclusions

HTS magnetic bearing technology for pre-industrial use has been demonstrated up to loads of 10 kN. A 5 kWh / 250 kW HTS flywheel with total magnetic stabilization of the 0.6 t rotor was assembled and tested. With HTS magnetic flywheel improvements increased storage efficiency can be achieved. PM – HTS coupling technology over large distance of 10 – 15 mm allows to perform chemical processes with semiconductors under extreme processing conditions while rotating. A magnetic coupling system for semiconductor wafer treatment has been constructed. Superconducting MAGLEV demonstrators with 0.25 t load performance and long - time LN_2 cooling operation is presented and successfully tested for use of a future MAGLEV train. With increased magnetic flux density much higher forces and loads of SMB systems become possible.

References

[1] F. C. Moon a. P. Z. Chang; “High-speed rotation of magnets on high Tc superconducting bearings”,Appl. Phys. Lett. 56(1990)397-399.

[2] R. Weinstein, I. G. Chen , J. Liu, and K. Lau, „Permanent magnets composed of high temperature superconductors”, J. Appl. Phys. 70 (1991)6501–6503.

[3] M. Murakami,” Melt Processed High-Temperature Supercond.” (1992) Singapore: World Scientific.

[4] J. R. Hull, “Superconducting Bearings”, Supercond. Sci. Technol. 13 (2000) R1 - R15.

[5] G. Ries u. F. Werfel, „In der Schwebe“ , Phys. Unserer Zeit, Nr. 3/2004, S. 134-140, Wiley VCH Verlag Weinheim.

[6] A. Day, J. Hull, M. Strasik, P. E. Johnson, K. E. McCrary, J. Edwards, J. A. Mittleider, J. R. Schindler, R. A. Hawkins, M. L. Yoder, „Temperature and Frequency Effects in a High – Performance Superconducting Bearing, “,IEEE Trans. Appl. Supercond., Vol. 13, No. 2 (2003), 2179-2184.

[7] T. Ichihara, K. Matsunaga, I. Hirabyashi, M. Isono,, M. Hirose, K. Yoshii, K. Kurihara, O. Saito, M. Murakami, H. Takabayashi, M. Natsumeda, N. Koshizuka, “Application of Superconducting Magnetic Bearings to a 10 kWh-Class Flywheeel Energy Storage System“, IEEE Trans. Appl. Supercond., Vol. 15, No 2 (2005) 2245-2248.

[8] F. N. Werfel, U. Floegel – Delor, T. Riedel, R. Rothfeld, D. Wippich, B. Goebel, G. Reiner, and N. Wehlau “A Compact HTS 5 kWh/250 kW Flywheel Energy Storage System”, IEEE Trans. Appl. Supercond. Vol.17, No.2 (2007)2138-2141.

[9] J. S. Wang, S. Y. Wang, Z. Y. Ren, M. Zhu, H. Jiang, Q. X. Tang, “Levitation force of a YBaCuO bulk high temperature superconductor over a NdFeB guideway”, IEEE Trans. Appl. Supercond. 11, 1 (2001)1801 – 1804.

[10] G. G. Sotelo, D. H. N. Dias, O. J. Machado, E. D. David, R. de Andrade Jr., R. M. Stephan, G. C. Costa, ”Experiments in a Real Scale MagLev Vehicle Prototype”, EUCAS’09, Sept. 13-17, 2009 Dresden, Germany.